TETRAGONAL LAYERED COMPOUNDS WITH VANADYL PHOSPHATE STRUCTURE AND THEIR INTERCALATION REACTIONS

Ludvík BENEŠ and Vítězslav ZIMA
Joint Laboratory of Solid State Chemistry
of Academy of Sciences of the Czech Republic and University of Pardubice

Intercalation reactions of vanadyl phosphate, niobyl phosphate, vanadyl arsenate, and vanadyl sulphate are summarized. In the review, the intercalations of molecular guests (water, alcohols, amines, carboxylic acids, amides, heterocycles, and metallocenes) and ions (alkali metals, divalent metals, and alkylammonium ions) are described. Layered compounds derived from vanadyl phosphate dihydrate, in which a part of vanadyl group is replaced by trivalent metal (Al, Cr, Fe, Ga, Mn), are mentioned.

Introduction

Intercalates are a special type of the inclusion compounds which are formed by the insertion of molecules or ions into empty sites between the layers of a layered lattice. All intercalation reactions are accompanied by a partial or total transfer of the charge to the lattice and cause a change of the interlayer distance (basal spacing). The molar ratio need not necessarily be the ratio of integer numbers.

The first intercalates were prepared 150 years ago, and the first host

lattice was graphite. Graphite is the only material which permits the intercalation of molecules without a lone electron pair or with a deficiency of electrons.

Other host lattices have been used from the beginning of the sixties. The most extensively investigated lattices for these processes are the chalcogenides of the transition metals of the type MX_2 (M = Ti, Nb, Zr, Hf, Sn, X = S, Se, Te), hydrogenphosphates $M^{IV}(HPO_4)_2$ (M = Zr, Sn, Ti) or their hydrates, lamellar oxide halides of transition metals of the type $M^{III}OCl$ (M = Fe, Cr), layered oxides (MO_3, WO_3), metal phosphorus chalcogenides $M^{II}PS_3$ (M = Cd, Ni, Zn, Mn), layered minerals (montmorillonite, beidellite etc.), vanadyl and niobyl compounds of the type $VOXO_4$ or $NbOXO_4$ (X = S, P, As).

The Structure of Vanadyl Phosphate

The structure of $VOPO_4.2H_2O$ determined by neutron diffraction[1] is tetragonal with space group P4/n and can be described as consisting of layers build up of PO_4 tetrahedra linked to VO_6 octahedra by sharing the phosphate oxygen atoms. The PO_4 tetrahedra are slightly flattened in the c direction, the VO_6 octahedra show a somewhat greater distortion. Two water molecules intercalated into the van der Waals gap between the $VOPO_4$ layers provide the necessary interlayer bonding.

The space group P4/nmm, reported for $VOPO_4.2H_2O$ on the basis of X-ray diffraction[2], differs from P4/n found by neutron diffraction. This difference is due to the limited ability of the X-ray diffraction method to find reliably the hydrogen positions. As it follows from the neutron diffraction data[1], the water molecules are slightly disordered in the following way: the first molecule is coordinated to the vanadium atom with two possible orientations and the second one can occupy two possible positions, creating the H-bridges either with the upper or lower phosphate oxygens (Fig. 1).

An anomalous thermal behaviour of the vanadyl phosphate dihydrate has been found in the temperature range of 3 - 42 °C, where the c-parameter decreases with increasing temperature, whereas the a-parameter remains constant[3]. Based on the temperature dependence of the lattice parameters and diffraction line profiles, the structural changes with variation of the temperature were derived and the mechanism of the topotactic dehydration proposed. It is evident that the interlayer hydrogen bonds play key role in the observed effect. This confirms common structural features of ices and hydrates and illustrates the influence of the crystalline environment on the behaviour of the water-water dimer.

Several modifications of anhydrous vanadyl phosphate are known[4,5]. One of them, $\alpha_1 - VOPO_4$ modification, is formed by the thermal dehydration of $VOPO_4.2H_2O$. The structure of the $VOPO_4$ layers remains unchanged, the coordination polyhedron of the vanadium atom is completed by the oxygen from the neighbour layer. $\alpha_1 - VOPO_4$ is isostructural with a number of other compounds including $\alpha_1 - VOSO_4$ (Ref.[6]), $VOAsO_4$ (Ref.[7]), and $NbOPO_4$

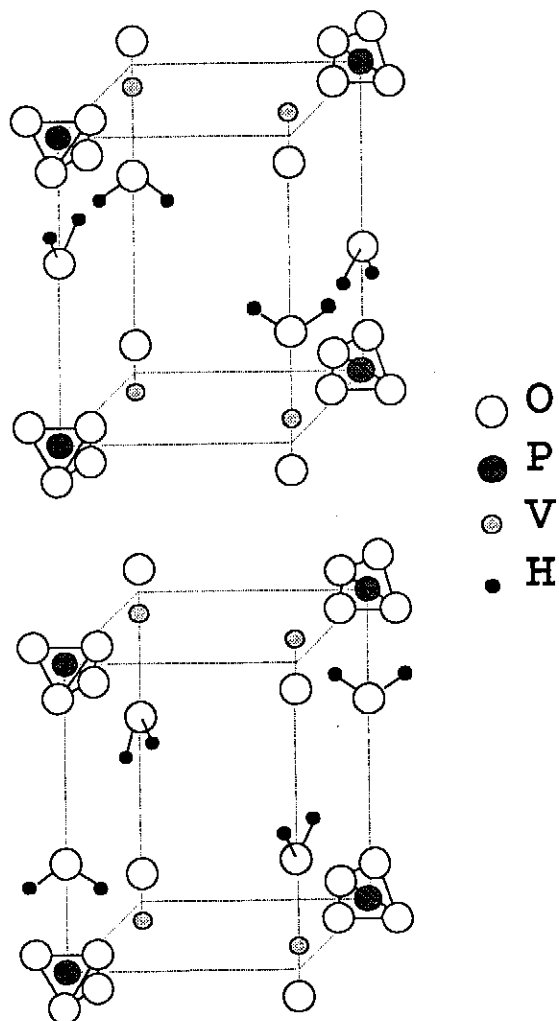Fig. 1 Two possible orientations of water moleculs in the $VOPO_4.H_2O$ structure (proposed by Tachez[1])

(Ref.[8]). The lattice parameters of the above-mentioned compounds are given in Table I.

If foreign molecules penetrate into the structure of anhydrous vanadyl phosphate, the $(VOPO_4)_\infty$ layers stand apart and the sixth coordination position of the vanadium atom is occupied by a donor atom of the guest molecule. Vanadyl phosphate dihydrate, which can be considered as an intercalate of water into $VOPO_4$, may serves as an example.

Table I Lattice constants of tetragonal $MOXO_4 \cdot nH_2O$ compounds

Compound	a, Å	c, Å	Ref.
$VOPO_4 \cdot 2D_2O$	6.2154(2)	7.4029(7)	1
$VOPO_4 \cdot 2H_2O$	6.202(2)	7.410(1)	2
	6.210(2)	7.459(3)	3[a]
	6.210(2)	7.391(3)	3[b]
$VOPO_4 \cdot H_2O$	-	6.3	9, 11
$\alpha_1 - VOPO_4$	6.20	4.11	5, 9
	6.20	4.18	11
$\alpha - VOSO_4$	6.261(3)	4.101(3)	6
$VOAsO_4 \cdot 3H_2O$	6.39	8.08	7
$VOAsO_4 \cdot 2H_2O$	6.37	7.39	7
$VOAsO_4$	6.33	4.18	7
$NbOPO_4 \cdot 3H_2O$	6.39	8.04	10
$NbOPO_4 \cdot H_2O$	6.41	7.14	10
$NbOPO_4$	6.387(1)	4.104(1)	8

[a] at 3 °C
[b] at 42 °C

Intercalation and Deintercalation of Water into Vanadyl Phosphate

A course of dehydration of $VOPO_4 \cdot 2H_2O$ has been studied thoroughly by X-ray diffraction, thermomechanical analysis (TMA), DTA, and thermolectric power measurements[11].

The X-ray diffractograms of $VOPO_4 \cdot 2H_2O$ at the temperatures from 19 to 250 °C are given in Fig. 2. Three diffracting phases are present consecutively in the sample during heating. The basal spacing of these phases corresponds to values for $VOPO_4 \cdot 2H_2O$ (7.4 Å), $VOPO_4 \cdot H_2O$ (6.3 Å) and $VOPO_4$ (4.2 Å). The transformation of the dihydrate to the monohydrate occurs mainly about the temperature of 43 °C. The practically pure monohydrate is present at 63 °C. The second dehydration follows at about 80 °C, and the monohydrate is almost absent about 114 °C.

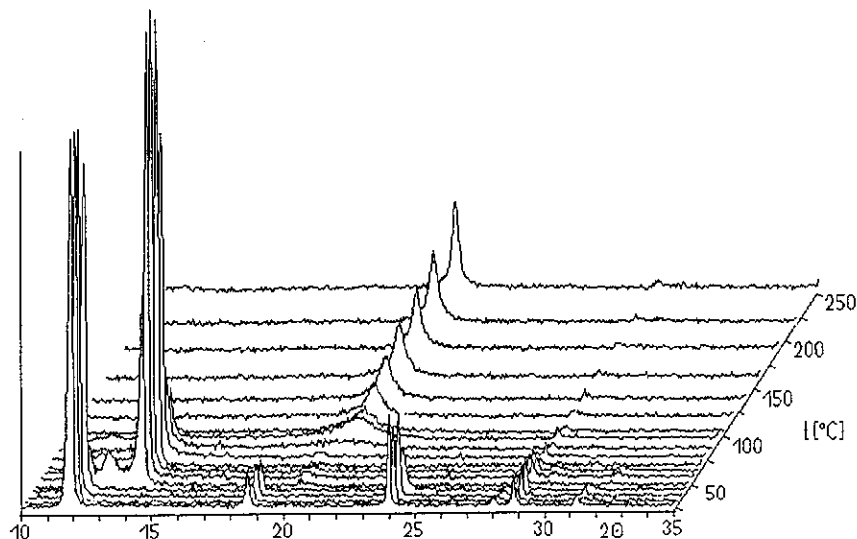The thermomechanical measurements (the change of thickness of the

Fig. 2 Temperature dependence of X-ray diffractograms (CuKα radiation) of $VOPO_4 \cdot 2H_2O$ (Ref.[11])

crystal across the layers during heating) show an evident two-step mechanism of dehydration. These steps are very sharply distinct (Fig. 3). The maximum change of the thickness of the crystal during the first dehydration step occurs at 44 °C and is followed by a region of constant thickness. The second dehydration step exhibits the maximum change at 79 °C. The end of the second dehydration is slower, with an exponential course. The temperatures of dehydration determined by TMA correspond to the values observed by X-ray.

A two-step loss of water has been observed by DTA measurements. Both temperatures of dehydration are higher in comparison with XRD and TMA. This discrepancy was explained by the fact that the released water is absorbed on the surface of the crystals and evaporates at the higher temperatures.

Thermoelectric power of the $VOPO_4 \cdot 2H_2O$ pellet in the temperature region from -75 to 150 °C is shown in Fig. 4. The temperature given on x-axis corresponds to the mean value between the electrodes with 15 °C gradient. Two decreases of the value of the Seebeck coefficient correspond to two-step dehydration of $VOPO_4 \cdot 2H_2O$. The sign of the Seebeck coefficient at temperature below 88 °C indicates that the predominant charge carriers are positive. The charge carriers are probably protons created by dissociation of water in the van der Waals band. The Seebeck coefficient is negative at higher temperatures, because electrons in anhydrous $VOPO_4$ become the predominant charge carrier.

The course of intercalation of water into $\alpha_1 - VOPO_4$ has been studied by the thermomechanical analysis and X-ray diffraction[12].

While dehydration of $VOPO_4 \cdot 2H_2O$ has a two-step mechanism, as it is shown above, hydration of anhydrous $\alpha_1 - VOPO_4$ followed by the thermo-
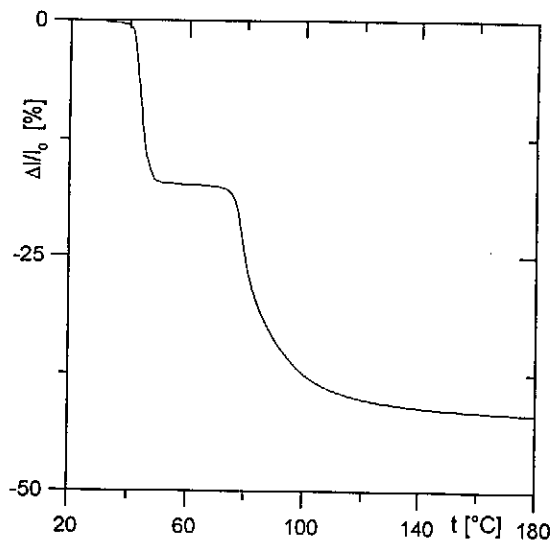
Fig. 3 Temperature dependence of the relative change of the thickness of the crystal measured across the layers of $VOPO_4.2H_2O$ (Ref.[11])
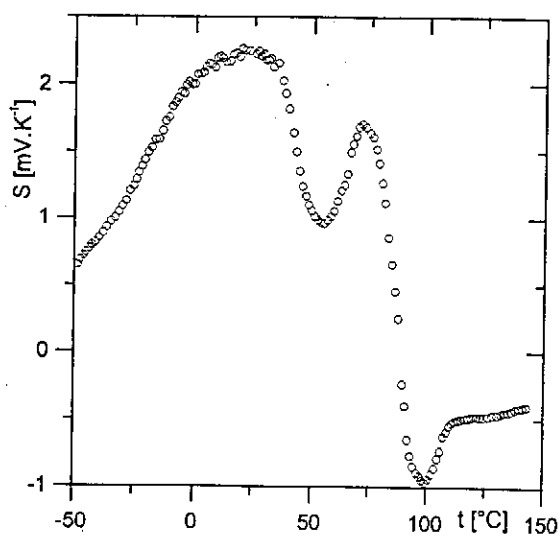

Fig. 4 Temperature dependence of Seebeck coefficient S of $VOPO_4.H_2O$ according to Ref.[11]

mechanical analysis occurs in one step. The dependence of the thickness of the crystal on time during hydration had an exponential shape. No significant dwell corresponding to a monohydrate formation or staging was observed.

The changes of the diffractograms during intercalation of water into α_1-VOPO_4 are given in Fig. 5. The original α_1-VOPO_4 (the lines denoted by

index a) is changed to $VOPO_4.2H_2O$ (the lines denoted by b). The lines of vanadyl phosphate monohydrate were not observed during hydration. During intercalation, the broadening and the shift of the positions of the (00l) lines were observed. These phenomena can be explained by the random stacking of the intercalated and nonintercalated layers in the sample. Then molecules of water probably fill the interlayer space randomly, creating a Hendricks-Teller disordered layer lattice, which is composed of the α_1-VOPO_4 and $VOPO_4.2H_2O$ layers.
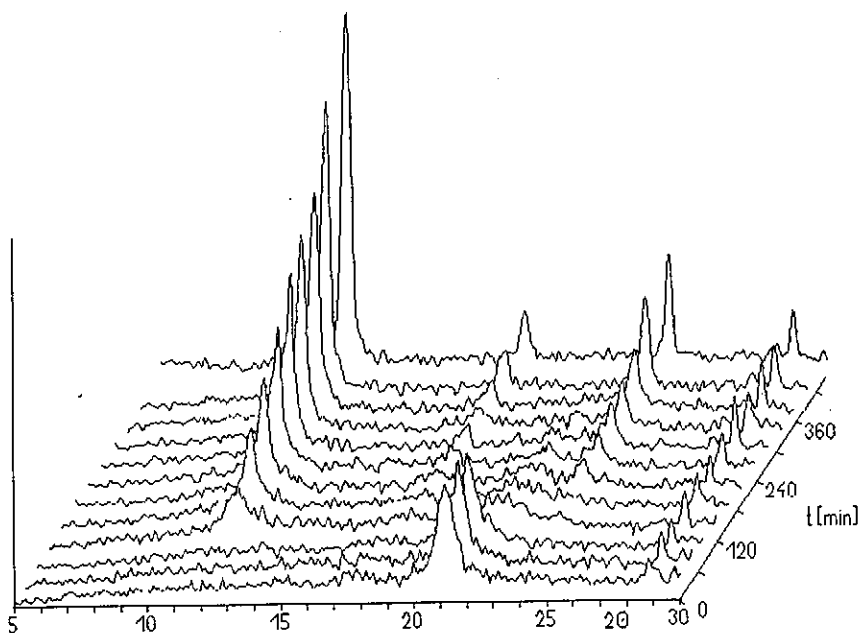

Fig. 5 The time changes of the X-ray diffractograms (CuKα radiation) during intercalation of water into anhydrous vanadyl phosphate[12]

The dependence of the water content and the basal spacing on relative humidity at 25 °C for $VOPO_4$ and $NbOPO_4$ have been determined[13]. Anhydrous vanadyl phosphate is stable when relative humidity is equal to zero, vanadyl phosphate dihydrate exists in the region of relative humidity between 15 to 50 %, and highly hydrated (10.5 Å) phase (denoted as $VOPO_4.5H_2O$) has been observed at relative humidity above 72 %. It is worth noticing that the monohydrate has no distinct region of the occurrence. Under relative humidity of 15 %, $NbOPO_4.H_2O$ is formed and $NbOPO_4.3H_2O$ exists at relative humidity higher than 45 %.

Beneš L., Zíma V./Sci. Pap. Univ. Pardubice Ser. A 2 (1996) 121-149

127

Intercalation of Alcohols into Vanadyl Phosphate and Sulphate

First examples of intercalation of alcohols into the $VOPO_4$ and $VOSO_4$ structure are given in Refs[9,14]. Recently, these systems have been studied in more detail[15]. The corresponding intercalates were prepared by reaction of the anhydrous hosts with an excess of liquid alcohol. The composition and lattice parameters of the complexes $VOSO_4.nROH$ and $VOPO_4.nROH$ are shown in Tables II and III. All $VOSO_4.nROH$ intercalates are light blue in color. Alcohols are readily liberated in air and are replaced with water. The $VOPO_4.nROH$ intercalates are yellow-green microcrystalline compounds with extreme sensitivity to humidity. No alcohols higher than C_4 can be intercalated by this method.

Table II Composition and tetragonal lattice parameters of $VOSO_4.nC_qH_{2q+1}OH$ intercalates[15]

Alcohol	n	n, Å	c, Å
CH_3OH	1.33	6.35	8.04
CH_3CH_2OH	2	6.34	12.84
$CH_3(CH_2)_2OH$	2	6.35	14.42
$(CH_3)_2CHOH$	1.75	6.34	13.33
$CH_2=CHCH_2OH$	2	6.35	14.73
$CH_3(CH_2)_3OH$	2	6.35	17.77
$(CH_3)_2CHCH_2OH$	1.75	6.35	14.83
$CH_3CH=CHCH_2OH$	2	6.34	18.31
$CH_3(CH_2)_4OH$	2	6.34	19.65
$(CH_3)_2CH(CH_2)_2OH$	1.75	6.34	17.15
$CH_3(CH_2)_5OH$	2	6.33	22.48
$CH_3(CH_2)_6OH$	2	6.34	24.57
$CH_3(CH_2)_7OH$	2	6.34	27.63

The lattice parameter (c_q) varies with the number of carbon atoms q in the alkyl chain ($CH_3(CH_2)_{q-1}OH$, $q = 1$ to 8). The increase of the basal spacing alternates regularly according to the relationship

$$c_q - c_{q-1} < c_{q+1} - c_q \quad \text{with} \quad q = 2r+1, \quad r = 0, 1, 2, ..., n$$

Table III Composition and lattice parameters of $VOPO_4 \cdot nC_qH_{2q+1}OH$ intercalates[15]

Alcohol	n	a, Å	c, Å
CH_3OH	1.33	-	7.85
CH_3CH_2OH	2	6.22	13.17
$CH_3(CH_2)_2OH$	2	-	14.40
$CH_3(CH_2)_3OH$	2	-	17.96

The basal spacings increase by about 0.32 nm from q = even number to $q + 1$ (except methanol) and by about 0.17 nm from q = odd number to $q + 1$. The increase of the lattice parameter after intercalation of the alcohols into both hosts corresponds to a bilayer arrangement of the alcohol molecules. The found alternation of the basal spacings with the number carbon atoms of the chain is explained by the fact that the chains are tilted under the angle of about 55°. An example of the proposed bilayer chain aggregation in $VOSO_4 \cdot 2C_4H_9OH$ is given in the Fig. 6.
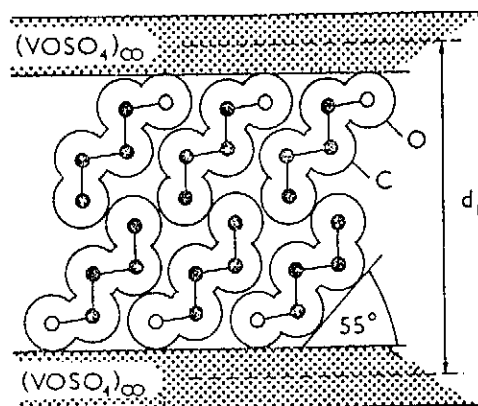

Fig. 6 Bilayer chain aggregation in $VOSO_4 \cdot 2C_4H_9OH$. Reproduced with permission from Inorg. Chim. Acta[18]

When branched alcohols are intercalated, the molar ratio of the alcohol to the host material is reduced (n = 1.75). This is obviously caused by sterical reasons. The intercalates with methanol show the lowest content of alcohol (n = 1.33) and the basal spacing indicates a monolayer of methanol molecules.

A study of rate of the intercalation of alcohols into these hosts has been carried out by a volumetric method[16]. This method is based on the fact that a closed heterogeneous system formed from a polycrystalline host and a liquid molecular guest decreases its volume during the intercalation process. The method was used to estimate the time course of intercalation of 1-butanol into $VOSO_4$

at various temperatures and intercalation of ethanol with various content of water into $VOPO_4$. The rate of intercalation of n-butanol into $VOSO_4$ increases with increasing temperature. The value of activation energy E_a = 54.6 kJ mol^{-1} has been determined. The rate of the intercalation process could be influenced by the moisture in the liquid guests. A very distinct effect of this kind was observed in the system $VOPO_4$ and wet ethanol, in which a strong acceleration of the reaction was observed.

The temperature dependence of sorption of vapours of three aliphatic alcohols (ethanol, 1-propanol, 1-butanol) into anhydrous vanadyl sulphate has been measured[17]. The host was used as a packing in a gas chromatographical column.

The mixed intercalates of the $VOXO_4 . (2-x)C_pH_{2p+1}OH . xC_qH_{2q+1}OH$ (X = S, P) type have been prepared by the reaction of anhydrous $VOXO_4$ with liquid binary mixtures of the unbranched alcohols[18,19]. The relations between the basal spacings of the intercalates formed, their composition and the composition of the liquid alcohol mixtures (C_2 to C_7 for $VOSO_4$ and C_1 to C_4 for $VOPO_4$) were studied.

The dependence of the basal spacings of all the solid phases prepared on the composition of the starting alcohol mixtures have a characteristic form for all the systems of the alcohols (except for the mixtures with methanol), the carbon chains of which differ by more than two carbon atoms. These curves can be divided into three parts (Fig. 7). The part marked R corresponds to the region of the practically pure $VOXO_4 . 2C_p$ (C_p denotes an alcohol with shorter chain). The mixed intercalates formed in the region S correspond to the formula $VOXO_4 . C_p . C_q$. The arrangement of the alcohol molecules in such a mixed intercalate is given in Fig. 8. The intercalates $VOXO_4 . (2-x)C_p . xC_q$ (x = 1.75 - 2) form a solid phase in the T region. However, the content of the alcohol C_p clearly increases in the solid phase with its increasing concentration in the liquid alcohol mixture. Therefore, in the T region the slope of the curve never becomes zero and its course is different from that in the R region.

Comparison of the widths of the R and T regions in all these investigated systems leads to the following conclusions:

The tendency to the penetration of the longer alcohols C_q into $VOSO_4 . 2C_2$ and the formation of the mixed intercalates is given by the order $C_7 > C_6 = C_5 > C_4$.

The order $C_2 > C_3 > C_4 > C_5$ expresses how easily the alcohol with a shorter carbon chain penetrates into the intercalates $VOSO_4 . 2C_6$ and $VOSO_4 . 2C_7$ to form the mixed intercalates. Similarly, for the penetration of the shorter alcohols into $VOSO_4 . 2C_5$ the order is $C_2 > C_3$.

A different behavior has been observed in the systems of $VOPO_4$ with a mixture of methanol with longer alcohols[19]. The intercalate $VOPO_4 . 1.33C_1$ is formed even at high content of the longer alcohol (30 % for ethanol, 70 % for propanol, and 91 % for butanol) in the mixture. At higher content of the longer alcohol in the mixture, an intercalate with the formula $VOPO_4 . (2-y)C_1 . yC_q$ is
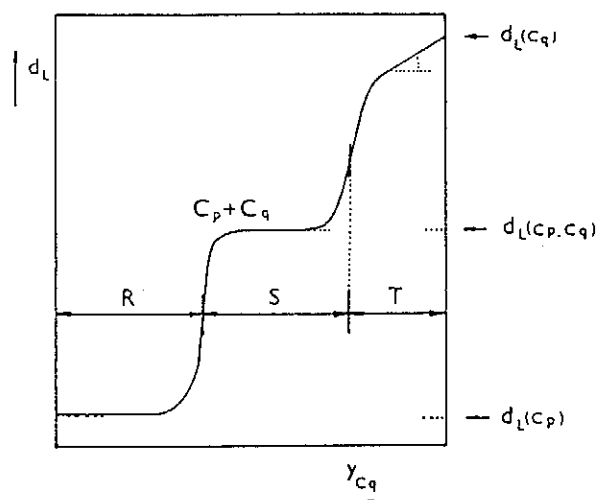
130

formed.

Fig. 7 A typical curve of the basal spacing dependence on the composition of the liquid binary alcohol mixture (C_p and C_q) if aliphatic chains of the alcohols differ by at least two carbon atoms. The values of the basal spacing of $VOSO_4.2C_p$ and $VOSO_4.2C_q$ are denoted as $d_L(C_p)$ and $d_L(C_q)$; $d_L(C_p, C_q)$ is the basal spacing of the mixed intercalate. R, S, and T are regions of the existence of these three intercalates. Reproduced with permission from Inorg. Chim. Acta[18]
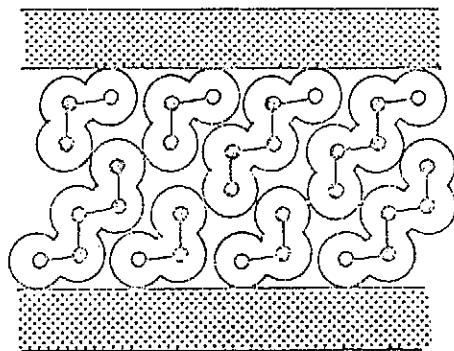

Fig.8 The arrangement of alcohol molecules in the mixed intercalate $VOSO_4.EtOH.BuOH$. Reproduced with permission from Inorg. Chim. Acta[18]

Intercalation of Amines into Vanadyl and Niobyl Phosphate

Aliphatic amines from C_4 to C_{16} have been intercalated into $NbOPO_4.3H_2O$ and $VOPO_4.2H_2O$ (Ref.[13]). The dependence of the basal spacing on the number

of carbon atoms is nearly linear and the interlayer distance indicates the angle of about 60° between the carbon chain and the plane of the layer for the chains up to C_{11}. The longer chains have perpendicular orientation. The composition of these intercalates is $MOPO_4.H_2O.1.5RNH_2$ (M = V, Nb). The basal spacings of the intercalates of some other amines into $NbOPO_4.H_2O$ are given in Table IV.

Table IV Basal spacing of $NbOPO_4.3H_2O$ intercalated with amines[13]

Amine	Basal spacing, Å
di-n-butylamine	21.6
2-aminobutane	22.0
(3-methylbutyl)amine	19.0
methylbutylamine	22.4
methyl-sec-butylamine	21.3
methyl-isobutylamine	22.1
dimethylbutylamine	21.7
4-amino-2-butanol	6.2
ephedrine	24.8
cyclohexylamine	14.7
aniline	26.0

The intercalates of anhydrous $VOPO_4$ and aliphatic amines with an unbranched chain C_1 to C_{10} were obtained by the direct reaction[20]. Preparation conditions, basal spacings, and composition of $VOPO_4.xC_nH_{2n+1}NH_2$ are given in Table V. The basal spacings increase by about 1.4 Å when extending the chain from n = even number to $n + 1$ and by about 3.1 Å from n = odd number to $n + 1$. This alternation indicates the bilayer arrangements of the molecules, which are inclined at the angle of 55° to the layer of host. This angle increases slightly with the increasing number of the carbon atoms in the chain. The number of the molecules x_1 of amine in the intercalate (see Table V) was calculated as a ratio of the difference between the unit cell volume of the intercalate and anhydrous $VOPO_4$, and the molar volume of the amine, which was calculated from its density at the melting point.

Due to the possibility to reduce vanadium atom, redox intercalations of alkylammonium ions into $VOXO_4.nH_2O$ (X = P, As) carried out[21]. These hosts react with alkylammonium iodides in acetone solution to form $(RNH_3)_xV_x^{IV}V_{1-x}{}^VOXO_4.yH_2O$; the composition and the basal spacing of the products are given in Table VI. The "pillar" arrangement of the alkyl chains is

presumed.

Table V Preparation conditions, composition, and lattice parameters of $VOPO_4$ with amines[20]

Amine	Preparation		Basal spacing c	Composition	
	T °C	time min	Å	x_1(XRD)	x_2(DTA)
CH_3NH_2	-33	5	10.903	2.02	-
$CH_3CH_2NH_2$	7	30	13.523	1.95	-
$CH_3(CH_2)_2NH_2$	20	120	14.593	1.70	-
$CH_3(CH_2)_3NH_2$	20	20	18.33	1.84	1.92
$CH_3(CH_2)_4NH_2$	20	300	19.80	1.78	2.09
$CH_3(CH_2)_5NH_2$	20	180	22.91	1.72	1.95
$CH_3(CH_2)_6NH_2$	60	30	24.31	1.72	2.16
$CH_3(CH_2)_7NH_2$	60	60	27.71	1.86	1.82
$CH_3(CH_2)_8NH_2$	60	120	29.16	1.68	2.18
$CH_3(CH_2)_9NH_2$	100	15	31.71	1.94	1.92

Similarly, powdered $VOPO_4.2H_2O$ suspended in an excess of neat aniline gives intercalation compounds $VOPO_4.xH_2O.yC_6H_5NH_3^+$ ($0.6 < x < 1.1$; $0.5 < y < 1.0$) with the vanadium atoms reduced[22]. Two phases were observed ($d = 15.0$ Å, $d = 9.0$ Å) during intercalation. Addition of the Cu^{2+} ion leads to polymerization of the cation and polyaniline is formed. Suspended $VOPO_4.2H_2O$ powders react with $C_6H_5NH_3^+Cl^-$ dissolved in ethanol to give the compound intercalated with both the anilinium cation and polyaniline.

Intercalation of Carboxilic Acids into Vanadyl Phosphate, Sulphate and Arsenate

Layered complexes $VOXO_4.RCOOH$ (X = P, As, S; RCOOH means formic, acetic, propionic and butyric acids) have been prepared[23]. The intercalates are formed either by the intercalation reaction of the anhydrous host lattice with liquid carboxylic acids or by the exchange reactions of the hydrates $VOXO_4.nH_2O$ or the intercalates $VOXO_4.2C_2H_5OH$ with acids in the presence of a dehydrating agent.

Beneš L., Zima V./Sci. Pap. Univ. Pardubice Ser. A 2 (1996) 121-149

133

Table VI Basal spacing (*d*) and composition of intercalation compounds $(RNH_3)_xVOXO_4 \cdot yH_2O$ (Ref.[21])

R	Phosphates (X = P)			Arsenates (X = As)		
	x	*y*	*d*, Å	*x*	*y*	*d*, Å
$n-C_3H_7$	0.5	1.0	14.6	0.4	1.0	14.4
$n-C_4H_9$	0.5	1.0	17.0	0.4	1.0	16.4
$n-C_6H_{13}$	0.4	1.0	18.8	0.5	1.0	18.5
$n-C_7H_{15}$	0.5	1.0	19.2	0.5	1.0	19.2
$n-C_8H_{17}$	0.6	1.1	22.1	0.5	1.0	21.3
$C_6H_5CH_2$	0.5	0.8	17.5	0.4	0.9	16.3

The lattice parameters and decomposition temperatures of the intercalates are given in Table VII. It is obvious that the dependence of the basal spacing on the number of carbon atoms in carboxylic acids is identical for all three hosts. The basal spacing is changed by about 1.8 Å when going from the

Table VII Lattice parameters ond decomposition temperatures of tetragonal $VOXO_4 \cdot RCOOH$ compounds[23]

Host	Quest	Decomposition temperature °C	Lattice parameters	
			a, Å	*c*, Å
$VOPO_4$	HCOOH	170	6.21	7.19
	CH_3COOH	190	6.22	8.96
	$n-C_2H_5COOH$	250	6.23	9.37
	$n-C_3H_7COOH$	-	6.22	11.42
$VOAsO_4$	HCOOH	190	6.21	7.19
	CH_3COOH	215	6.22	8.96
	$n-C_2H_5COOH$	-	6.23	9.37
$VOSO_4$	HCOOH	140, 235	6.21	7.19
	CH_3COOH	170	6.22	8.96
	$n-C_2H_5COOH$	-	6.23	9.37

complexes with formic acid to those with acetic acid, and the change is the same (2.0 Å) when going from propionic to butyric acid. On the other hand, when replacing acetic acid by propionic acid we find an increase of only 0.2 - 0.4 Å in the basal spacing. This phenomenon can be explained by an oblique arrangement of the chains, which is schematically represented in Fig. 9. The figure gives the differences of the basal spacings between the intercalate and the anhydrous host calculated for the location of one layer of carboxylic acid molecules, which are tilted at an angle of 55°. For butyric acid, this difference is also determined with almost perpendicular orientation of its chain with respect to the host layers. For this simple calculation, the known values of C-H and C-C bond lengths and van der Waals radii of the hydrogen atom and carboxylic group were used. The differences calculated correspond very well to the results obtained from the diffractograms. From the IR spectra it follows that the carboxylic acid molecules are anchored by their functional group and that also a strong hydrogen bond obviously is present. The IR spectra do not contain any bands of the carboxylate ion, hence no proton transfer occurs from the carboxylic acids to the host lattice.
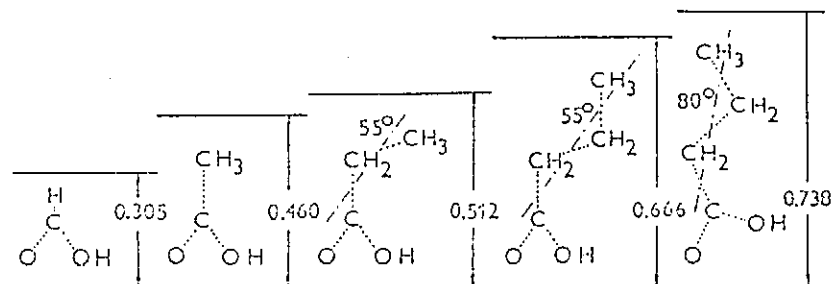

Fig. 9 Steric demands of molecules of aliphatic carboxylic acids deposited between host layers. The calculated distance value is given in nanometers. Reproduced with permission from Inorg. Chim. Acta[23]

Intercalation of Amides into Vanadyl Phosphate and Arsenate

The laminar compounds $VOPO_4.2H_2O$ and $VOAsO_4.3H_2O$ interact with primary and tertiary amides causing either dehydration or intercalation reactions, or sometimes both[24]. The tetragonal structure of the starting solids is preserved and in some cases mixtures of phases with different degrees of swelling can be seen. The compositions and the basal spacings of the vanadyl phosphate intercalates with amides are shown in Table VIII. In the case of the intercalates of vanadyl arsenate with amides the system contains more solid phases. The interaction between tertiary amides and the substrates is realized by the C=O and V-O groups, either directly or indirectly through the coordinated water, as it follows from the IR spectra. When the compounds are hydrated, the primary

amides also interact through the NH_2 groups to form hydrogen bridges. In the anhydrous compounds resulting from the reaction of formamide, refluxed with $VOPO_4 \cdot 2H_2O$ and $VOAsO_4 \cdot 3H_2O$, the amide coordinates directly with the vanadium through the NH_2 groups.

TableVIII Composition and basal spacing of $VOPO_4 \cdot xRCONH_2 \cdot yH_2O$ and $VOPO_4 \cdot xRCON(CH_3)_2 \cdot yH_2O$ intercalates[24]

Amide	Composition		Basal spacing Å
	x	y	
formamide	1.60	0.00	7.59
N,N-dimethylformamide	0.82	0.00	9.49
N,N-dimethylacetamide	0.34	0.25	7.37
acetamide	0.10	1.80	7.45
butyramide	0.00	2.00	7.40
benzamide	0.00	2.00	7.40

Intercalation of Heterocycles into Vanadyl Phosphate and Arsenate

Coordination intercalation compounds of $VOPO_4$ and $VOAsO_4$ with pyridine and 4-substituted pyridines are described in Ref.[25]. Preparation conditions, composition and lattice parameters are given in Table IX. The intercalation of pyridine expands the layer separation of $VOPO_4$ and $VOAsO_4$ by 5.5 Å. This is consistent with a bonding model in which pyridine is coordinated to vanadium with the ligand plane perpendicular to the layers. While it is difficult to predict exactly the c axes of these coordination intercalates without knowledge of the metal-ligand bond distance and the structural details of the layer itself, it can be assumed that these factors remain constant as the ligand size increases. Thus, the difference in the van der Waals length along the coordination axis between pyridine and 4-phenylpyridine can easily be measured and compared directly to the observed c axis differences. The 4.6 Å expansion observed when going from $VOPO_4 \cdot$ pyridine to $VOPO_4 \cdot (4-phenylpyridine)$ corresponds closely to the differences in the lengths of the ligands (4.4 Å). This indicates that, the pyridine molecules from adjacent layers interpenetrate in the $VOXO_4$ compounds, and the total expansion is then caused by a single ligand. On the $VOPO_4$ layer surface, the coordination sites are 6.2 Å apart. This is only a little less than the van der Waals width of pyridine (6.4 Å) allowing the ligands to line up along the a axis and stack in an interlocking fashion along the c axis. As it follows from the ESR spectra, there is no reduction of V^{5+} atoms during intercalation of pyridine.

Table IX Preparation conditions, composition and lattice parameters of the $VOPO_4 . xC_5H_5N$ intercalates[27]

Preparation conditions	x (TGA)	Lattice parameters	
		a, Å	c, Å
$VOPO_4 . 2H_2O$ + pyridine 10 days, reflux	0.97	6.207	9.589
$VOPO_4$ + dry pyridine 14 days, 100 °C, ampoule	0.36	6.21	9.1 - 9.6
$VOPO_4$ + dry pyridine 14 days, 125 °C, ampoule	0.82	6.216	9.566
$VOPO_4$ + dry pyridine 4 days, 150 °C, ampoule	0.75	6.21	9.51 - 9.58
$VOPO_4$ + dry pyridine 6 days, 150 °C, ampoule	0.87	6.21	9.47 - 9.56
$VOPO_4$ + dry pyridine 4 days, 170 °C, ampoule	0.85	6.20	9.51
$VOAsO_4$ + dry pyridine 10 days, 150 °C, ampoule	1.0	6.403	9.661
$VOPO_4$ + 4,4' - bipyridine 3 days, 110 °C, ampoule	0.5	-	13.0
in xylene 48 days, 200 °C	1.0	-	14.2

Intercalate have also been prepared by reaction of acetone solution of tetrathiafulvalene (TTF) with $VOPO_4 . 2H_2O$ at room temperature for 15 days[26]. The product has the composition of $VOPO_4 . H_2O . (TTF)_{0.25}$. The supposed layered structure has not been confirmed by XRD. The system is probably more complex than a simple intercalation of TTF into $VOPO_4 . 2H_2O$. The infrared spectrum indicates the presence of the TTF^+ radical in this material. The electrical properties of the product have been studied.

Finely powdered $VOPO_4 . 2H_2O$ suspended in an ethanol solution

containing 3-methyl- or 3,4-dimethylpyrrole leads to the intercalative polymerization of these pyrrole derivatives through the 2,5-coupling to yield $VOPO_4 \cdot (H_2O)_{1.4} \cdot (C_2H_5OH)_{0.2} \cdot (methylpyrrole)_{0.65}$ and $VOPO_4 \cdot (H_2O)_{1.8} \cdot (C_2H_5OH)_{0.2} \cdot (dimethylpyrrole)_{0.6}$ (Refs([27,28])). The similar treatment of $VOPO_4 \cdot 2H_2O$ with pyrrole affords polypyrrole only on the $VOPO_4$ surface.

Pyrrole almost completely polymerizes on intercalation into $VOPO_4 \cdot 2H_2O$, giving nestled polymer composites with differing polypyrrole oxidation levels, whereas aniline uptake is governed by base protonation and proton induced reassembly[29]. Calcinated $VOPO_4 (polypyrrole)_{0.66} \cdot 1.4H_2O$ (from neat pyrrole) is a semiconductor, the EPR spectra (cation amine and separated V^{IV} ions) further supporting strong polymer sheet electronic interaction with the formation of V^{IV} island clusters.

Under soft conditions (i.e. at ambient temperature in dry ethanol) pyrazole, pyrazine, and phenazine intercalate into $VOPO_4 \cdot 2H_2O$ as protonated, non-coordinated amines[29]. A bilayer structure is described in the case of pyrazine intercalate, while benzidine (bz) gives two charge transfer bronzes: $VOPO_4 (bz)_{0.5} \cdot 2H_2O$ (dry EtOH) and $VOPO_4 (bz)_{0.7} \cdot 3.5H_2O$ (95% EtOH) with interlayer distances surprisingly lower (7.05 and 6.65 Å, respectively) than in $VOPO_4 \cdot 2H_2O$ itself. Interlayer pocket orientation with layer shifting and turbostraticity to accommodate bz^+ cations is suggested, which differs from the assembly of bz^+ in smectites and V_2O_5.

Vanadyl phosphate dihydrate reacts with imidazole (Im) in anhydrous ethanol[30] to give a layered compound (basal spacing 10.3 Å), whereas in 95% ethanol it gives a phase with basal spacing 8.8 Å. Both compounds have the formula $VOPO_4 (Im)_{1.0} \cdot nH_2O$ (where n is 0.6 and 0.2, respectively).

Intercalation of Ferrocene into Vanadyl Phosphate

Ferrocene and its alkyl-substituted derivatives intercalate into the lamellar vanadyl phosphate, where ferricinium and related cation species are located in the interlayer space of the V^{IV}/V^V moieties. Two preparative methods were used.

The first of them consists in mixing of $VOPO_4 \cdot 2H_2O$ with ferrocene dissolved in acetone[31]. The mixture was stirred for several hours. In all samples, phases with the basal spacings of 9.9 Å and 8.5 Å were found. By heating of the sample to 100 °C, only the phase with the basal spacing of 8.5 Å was observed. An increment of the basal spacing indicates that ferrocene forms a molecular monolayer between the slabs of the host structure. Sterical arguments based on the size of the ferrocene molecule suggest that this guest lies with its fivefold symmetry axis parallel to the host layers. The observed IR absorption bands of intercalates correspond to vibration modes of the ferricinium ion. The content of ferricinium is relatively low (0.11 to 0.12 moles of guest to one mole of host). The corresponding part of vanadium atoms is reduced during reaction.

Second method of preparation[32] is based on the reaction of $VOPO_4 \cdot 2H_2O$ with an excess of ethanol, forming a mixed intercalate $VOPO_4 \cdot H_2) \cdot C_2H_5OH$. This compound was suspended in ethanolic solution of ferrocene and stirred for one week at ambient temperature. The $VOPO_4 \cdot H_2O \cdot (Cp_2Fe)_{0.35}$ intercalate with basal spacing 9.9 Å was formed. The increment of basal spacing corresponds to an arrangement in which cyclopentadienyl planes are parallel to the sheets of the host. The same basal spacing was found for a compound with a lower content of ferricinium ion $VOPO_4 \cdot H_2O \cdot (Cp_2Fe)_{0.21}$. By standing at room temperature, basal spacing of this compound changes to 8.8 Å. This is explained by a change of orientation of the ferricinium ions from parallel to perpendicular arrangement of cyclopentadienyl plane between sheets of the host.

Intercalation of Rhodium Carbonyl into Vanadyl Phosphate

Vanadyl phosphate dihydrate was intercalated by a $Rh_2(CO)_4Cl_2$ solution in tetrahydrofuran under argon at ambient conditions for 12 days[33]. The interlayer distance of the layered dark green solid prepared is 9.20 Å. The FTIR spectrum shows a broad band with distinct components centered at 2098 and 2107 cm^{-1}. The position of these bands is indicative of a Rh^I rather than a Rh^{III} carbonyl species in the intercalated compound. The catalytic activity and shape selectivity exhibited by the rhodium carbonyl species intercalated into a host compound with oxidation centers raises the very attractive possibility of such intercalated carbonyl species acting as novel catalysts.

Redox Intercalation of Mono- and Divalent Metal Cations into $VOPO_4 \cdot 2H_2O$

The reaction of crystalline $VOPO_4 \cdot 2H_2O$ with an ethanolic solution of MeI (Me = Li, Na, K, Rb, Cs, Mg, Mn, Co, Ni, Zn), which is rapid and spontaneous at room temperature, is a redox process[34]. The V^V atoms are reduced to V^{IV} by iodide, releasing iodine, and cations enter into the interlayer space simultaneously. The structure of the host layers is preserved during the reaction but the distance between adjacent $(VOPO_4)_\infty$ layers decreases. This decrease is due to the stronger interactions between the positively charged interlayer space and the negatively charged sheets of $VOPO_4$ with reduced vanadium atoms. The products are often composed from more phases, which differ by the basal spacing. The content of phases depends on the amount of the metal intercalated. This dependence for the sodium intercalates is given in Fig. 10. The phase composition for other metal intercalates is presented in Table X.

Hydronium ions cannot be intercalated into $VOPO_4$ by an analogous procedure to that used for above-mentioned cations because of the solubility of the host lattice in acid[35]. The reaction can be carried out using a nonaqueous
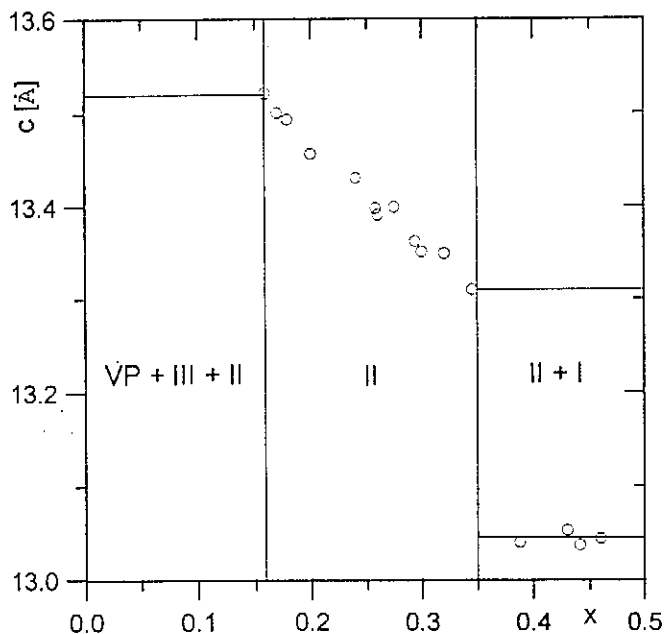
Fig. 10 Basal spacing vs. amount of intercalated sodium in $Na_xVOPO_4.2H_2O$ showing the regions of single-phase and two-phase behaviour according to Jacobson et at.[34]

solution of a hydrogen transfer agent such as hydroquinone forming $H_xVOPO_4.yH_2O$ ($0 < x < 1$). The water content (y is about 2.3) varied little with composition x. The products with $x < 0.26$ contained two phases whereas samples with $x > 0.26$ are apparently single-phase. However, a plateau observed in the interlayer separation as a function of the composition strongly suggests that there is a two-phase region centered on the composition of $x = 0.65$. By refluxing in 2-butanol, the intercalation compound is transformed to a blue layered crystalline phase which has the formula $VO(HPO_4).0.5H_2O$.

Redox intercalation of $VOPO_4.2H_2O$ with acetone solutions of LiI, NaI, KI, and hydroquinone were studied in more detail[36-39]. The time dependence of amount of the cation intercalated is exponential, and the rate of the reaction increases with increasing temperature.

A gradual creation of several solid phases has been observed. These phases correspond to the stages depicted in Fig. 11. Staging means a situation in the layer compounds in which certain galleries are filled, whereas others are empty[40]. The intercalate forms sequences in which empty galleries alternate with full gallery. The stages are numbered according to the number of the galleries in one sequence (the empty ones plus the full one). Two empty galleries and one full one gallery ($x = 0.33$) exist in stage 3, in stage 2 one empty gallery alternate with the full gallery ($x = 0.5$). Stage 1 consists only of the full galleries ($x = 1$).

Table X Intercalation compounds $Me_xVOPO_4 \cdot yH_2O$ (Refs[31,32])

Metal	x	y	a, Å	c, Å
lithium	1.0	2.0	6.350	12.811
	0.54	1.98	6.277	13.211
	0.4	2.14	6.265	13.293
			6.257	13.377
	0.23	2.33	6.231	14.168
potassium	0.64	1.51	6.300	12.752
	0.45	1.46	6.272	12.754
				13.530
	0.246	2.05	6.242	13.365
rubidium	0.52	1.62	6.280	12.943
	0.46	1.75	6.268	12.963
	0.239	1.82	6.246	13.407
cesium	0.13	-	6.226	13.860
	0.264	1.80	6.224	13.700
	0.309	-	6.246	13.620
	0.496	1.80	6.268	14.110
magnesium	0.22	3.63	6.27	6.62
	0.46	3.58	6.33	9.16
manganese	0.225	2.53	-	6.48
cobalt	0.25	2.35	6.28	6.59
nickel	0.235	2.31	6.27	6.61
zinc	0.30	2.56	6.28	6.63

In the case of sodium[36], the stage 3 is formed first, and only this phase is present in the system in a very short period, and so it is not possible to observe the kinetics of the stage 3 formation. Therefore, only a decrease in the stage 3 content is apparent (see Fig. 12), which is caused by a formation of stage 2. Consequently, the stage 2 is consequently replaced by the stage 1. The rate of this process increases with temperature. Fig. 13 shows the dependence of the basal spacing c and the relative content w_s of all three stages on the sodium content x in the solid reaction product. Values of the content of sodium x_s
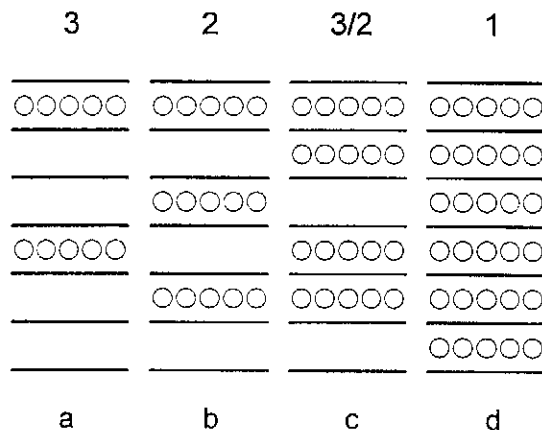
Beneš L., Zima V./Sci. Pap. Univ. Pardubice Ser. A 2 (1996) 121-149

141

Fig.11 Stages 3 (a). 2 (b), 3/2 (c), and 1 (d) of intercalated compounds according to (37). Solid line - the layers of $(VOPO_4)_\infty$; circles - the intercalated ions. Water molecules are omitted.

for all phases (Table XI) were determined by the multidimensional linear regression of the equation

$$x = \sum x_s w_s \tag{1}$$

where x is the total sodium content in the samples, and w_s is a relative content of the individual phases in the sample calculated from the equation

$$w_s = \frac{I_s(002)}{\sum I_s(002)} \tag{2}$$

where $I_s(002)$ is the intensity of the diffraction line (002) of the s-th phase. The water content determined by DTA remains constant up to $x = 0.5$. Above this value of x, the content of water decreases linearly. The content of water in stage 1 was calculated by the linear regression.

Similarly, during intercalation of lithium ions into $VOPO_4 \cdot 2H_2O$, four phases (stages) are formed[37]. Dependence of the relative content of phases w_s (calculated from Eq. (2)) on the lithium content x and their basal spacings are shown in the Fig. 14. The content of lithium in the individual phases was calculated in the same manner as in the case of sodium. The lattice parameters and the lithium contents of the individual phases are given in Table XII. In contrast to sodium, creation of a new phase is observed (with $x = 0.67$) between stages 2 and 1, which is out of the definition of the stages. The most plausible structure of this stage is a sequence of two full galleries and one empty (see Fig. 11c). The stage numbering, therefore, must be newly defined as a ratio

of the number of all the galleries (empty and full ones) to the number of the full galleries in each sequence. The stage mentioned is then denoted as a stage 3/2. This stage has not been observed in non-graphite intercalation compounds up to now. Numbering of the other stages is not changed in this way. The content of water is the same in all the four stages.
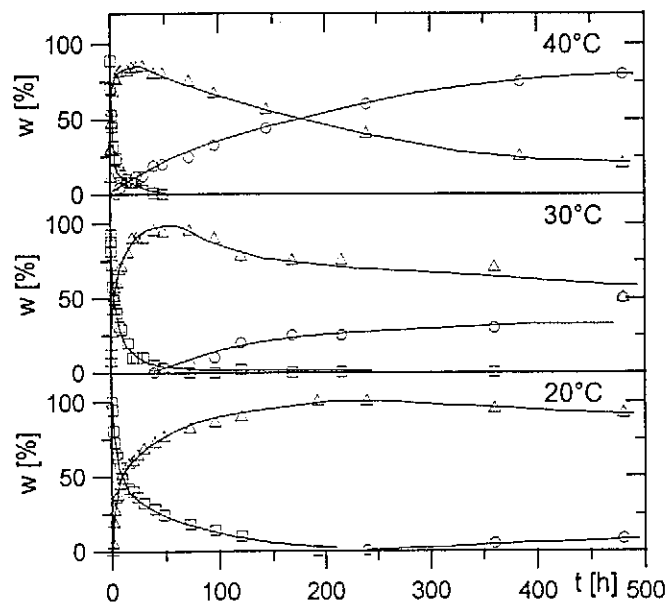

Fig. 12 Dependence of relative content w of the stages 3 (squares), 2 (triangles), and 1 (circles) in $Na_xVOPO_4 \cdot yH_2Ow$ on time t according to Ref.[36]

Table XI Composition and lattice parameters of $Na_xVOPO_4 \cdot yH_2O$ (Ref.[33])

Stage	x	y	a, Å	c, Å
3	0.30 ± 0.06	2.0 ± 0.1	6.240	13.370
2	0.50 ± 0.01	2.0 ± 0.1	6.284	13.063
1	1.07 ± 0.17	1.0 ± 0.1	-	11.330

In comparison with sodium and lithium the intercalation of potassium is a much slower process. To achieve almost fully intercalated product of $K_{0.97}VOPO_4 \cdot H_2O$, the shaking of the reaction mixture at 40 °C for 1600 hours is needed[39]. Several diffraction lines appear in the positions of the (001) lines again, which do not correspond to the (002) lines with sufficient precision. An exception is $K_{0.66}VOPO_4 \cdot H_2O$ with basal spacing 6.387 Å for all three reflections (001). The water content is close to 1, which was found out by DTA measurement for all the intercalates prepared.
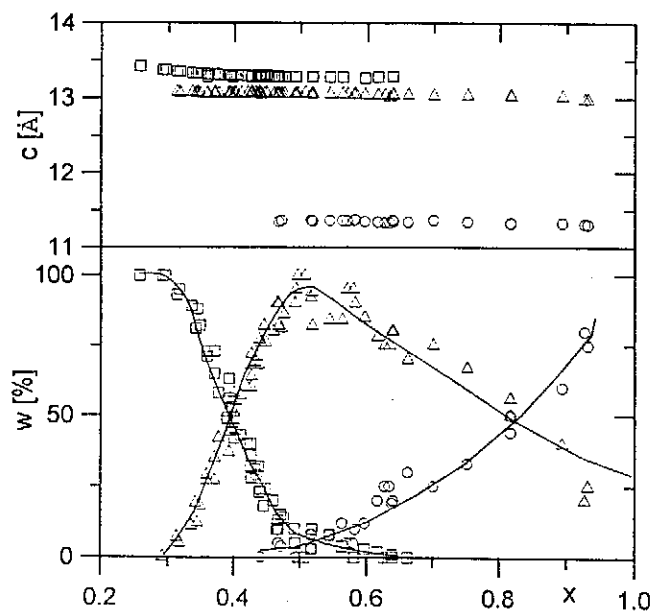
Fig. 13 Dependence of basal spacing c and relative content w of the stages 3 (squares), 2 (triangles), and 1 (circles) on sodium content x in $Na_xVOPO_4 \cdot yH_2O$ according to Ref.[36]

Table XII Composition and lattice parameters of $Li_xVOPO_4 \cdot 2H_2O$ (Ref.[34])

Stage	x	a, Å	c, Å
3	0.32 ± 0.03	6.230	13.361
2	0.49 ± 0.01	6.258	13.200
3/2	0.67 ± 0.01	6.284	13.055
1	1.01 ± 0.01	6.361	12.821

Hydronium intercalate has been prepared by intercalation of $VOPO_4 \cdot 2H_2O$ with acetone solution of hydroquinone[39]. This process is fast in comparison with intercalation of alkali metal ions (see above). The X-ray diffractograms of hydronium intercalates show a structure behaviour during intercalation similar to that of potassium intercalates. The water content in hydronium intercalates is increased during intercalation. This is explained by the fact that the hydronium ions enter the interlayer space as species which are solvated by water.

The conductivity behaviour of the redox intercalates mentioned, measured by impedance spectroscopy, is very similar[36-39]. The value of conductivity decreases with increasing content of guest (lithium, sodium, potassium and
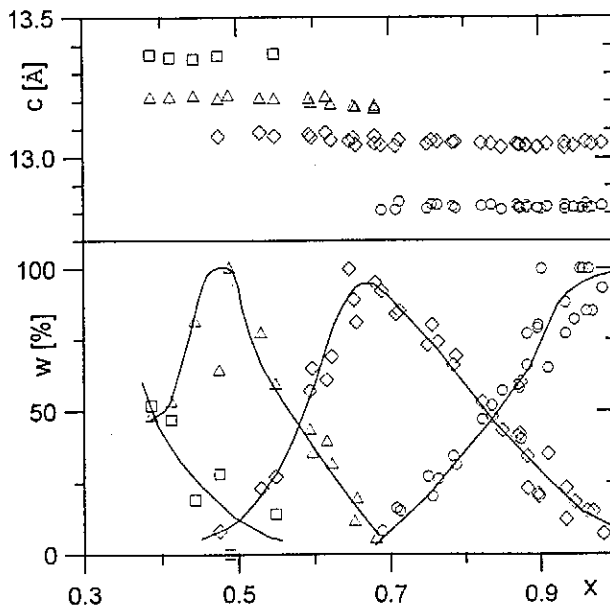
Fig. 14 Dependence of basal spacing c and relative content w of the stages 3 (squares), 2 (triangles), and 1 (circles) on sodium content x in $Li_xVOPO_4.2H_2O$ according to Ref.[37]

hydronium ions). The values of conductivity decrease almost linearly with increasing content of intercalated cation up to $x = 0.5$. At a higher content of guests, the conductivity remains almost constant. As it follows from the previous works[11, 41] the prevailing charge carriers in hydrates of vanadyl phosphate are positively charged. The only possible positively charged carriers are, in this case, protons from dissociation of the interlayer water. The decrease of conductivity is explained by the fact that the highest density of the negative charge after intercalation of cation is localized at the vanadium(IV) atoms. Intercalated positive charged species form counterparts of this negative charge. Therefore, cations intercalated are not so mobile as protons formed by dissociation of interlayer water.

Layered Compounds Derived from Vanadyl Phosphate by Partial Substitution of Vanadyl by Trivalent Metals

During the preparation of $VOPO_4.2H_2O$ according to Ladwig[9] in the presence of $KMnO_4$, a new tetragonal layered compound with formula $[Mn(H_2O)]_x(VO)_{1-x}PO_4.2H_2O$ ($x = 0.18 - 0.255$) was formed[42, 43]. Similarly, layered crystalline solids stable in air with general formula $[M(H_2O)]_x(VO)_{1-x}PO_4.2H_2O$ (M = Al, Cr, Fe, Ga; $x = 0.15 - 0.20$) have been

prepared by a reaction of solid V_2O_5 with boiling aqueous solution of phosphoric acid and corresponding metal salt[44]. The elementary cells of these compounds are tetragonal, space symmetry group either P4/n or P4/nmm, lattice parameters and densities are given in the Table XIII.

Table XIII The lattice parameters and densities of the substituted vanadyl phosphates

Formula	a, Å	c, Å	D_x, g cm^{-3}	D_o, g cm^{-3}
$[Al(H_2O)]_{0.15}(VO)_{0.85}PO_4.2H_2O$	6.202	14.066	2.390	2.47
$[Cr(H_2O)]_{0.17}(VO)_{0.83}PO_4.2H_2O$	6.219	13.710	2.486	2.50
$[Fe(H_2O)]_{0.20}(VO)_{0.80}PO_4.2H_2O$	6.221	13.686	2.500	2.58
$[Ga(H_2O)]_{0.18}(VO)_{0.82}PO_4.2H_2O$	6.216	13.700	2.531	2.66
	6.203	13.814	2.493	2.53

The structure of the compounds prepared is probably derived from the structure of $VOPO_4.2H_2O$ by substitution of a part of vanadyl groups $(VO)^{3+}$ by $[M(H_2O)]^{3+}$ ions as it follows from the XRD data. The substituting ions are built in the layers randomly, as it was observed from the magnetic susceptibility measurements of the paramagnetic ions. In these compounds, two molecules of water are intercalated in the same manner as in $VOPO_4.2H_2O$. In addition, every substituting ion coordinates one molecule of water to complete its coordination number to six.

Manganese-modified vanadyl phosphate has been submitted to reactions with selected liquid molecular guests[43]. This host also undergoes the redox intercalation with alkali metal ions, which was proved by reaction with sodium iodide. The preparation procedures used and the lattice parameters are listed in Table XIV.

Table XIV Synthesis and lattice parameters of intercalates of manganese-modified vanadyl phosphate with selected molecular guests and with sodium ions

Guest	Condition of synthesis			Lattice parameters	
	Preparation procedure	t °C	time	a Å	c Å
methanol	U	25	10 d	6.214	22.69[b]
				6.22	7.63[c]
ethanol	U	25	10 d	6.211	13.27
	R	40	1.0 h	6.288	13.044

Table XIV (Continued)

| Guest | Condition of synthesis | | | Lattice parameters | |
	Preparation procedure	t °C	time	a Å	c Å
n-propanol	H	25	8 d	6.216	14.463
n-butylamine	A	90	30 h	-	16.4
n-octylamine[d]	A	150	50 h	-	26.3
					23.8
					21.7
formic acid	H	25	7 d	6.217	7.209
acetic acid	H	25	10 d	6.199	9.083
pyridine	A	140	15 d	6.221	9.63
Na⁺	R	40	0.5 h	6.269	13.047
	R	40	1.0 h	6.288	13.044

[a] A ... anhydrous form of host with an excess of guest in a sealed pressure ampoule
  H ... dihydrate of host with an excess of guest
  U ... anhydrous form of host with an excess of guest
  R ... redox intercalation of dihydrate of host with acetone solution of NaI
[b] product is stable only in the presence of excess liquid methanol
[c] after washing with n-heptane
[d] three solid phases are formed

References

1. Tachez M., Theobald F., Bernard J., Hewat A.W.: Revue Chimie Minerale **19**, 291 (1982).
2. Tietze H.R.: Aust. J. Chem. **34**, 2035 (1981).
3. Čapková P., Vácha J. Votinský J.: J. Phys. Chem. Solids **53**, 215 (1992).
4. Jordan B., Calvo C.: Can. J. Chem. **51** 2621 (1973).
5. Bordes E.: These d'Etat, Compiegne (France), 1979.
6. Longo J.M., Arnott R.J.: J. Solid State Chem. **1**, 394 (1970).
7. Chernorukov N.G., Egorov N.P., Korshunov I.A.: Russ. J. Inorg. Chem. **23**, 1479 (1978).
8. Longo J.M., Kierkegaard P.: Acta Chem. Scand. **20**, 72 (1966).
9. Ladwig G.: Z. Anorg. Allg. Chem. **338**, 266 (1965).
10. Chernorukov N.G., Egorov N.P., Mocholova I.R.: Russ. J. Inorg. Chem. **23**, 1627 (1978).

Beneš L., Zima V./Sci. Pap. Univ. Pardubice Ser. A 2 (1996) 121-149

147

11. Zima V., Beneš L., Málek J., Vlček M.: Mat. Res. Bull **29**, 687 (1994).

12. Beneš L., Zima V.: J. Incl. Phenom. Mol. Recogn. Chem., **20**, 381 (1995).

13. Beneke K., Lagaly G.: Inorg. Chem. **22**, 1503 (1983).

14. Ladwig G.: Z. Chem. **20**, 70 (1980).

15. Beneš L., Votinský J., Kalousová J., Klikorka J.: Inorg. Chim. Acta **114**, 47 (1986).

16. Votinský J., Kalousová J., Beneš L., Baudyšová I., Zima V.: J. Incl. Phenom. Mol. Recogn. Chem. **15**, 71 (1993).

17. Baudyšová I., Votinský J., Beneš L., Kalousová J., Ventura K.: Sb. Věd. Prací, Vys. Škola Chem. Technol., Pardubice **53**, 21 (1989).

18. Votinský J., Beneš L., Kalousová J., Klikorka J.: Inorg. Chim. Acta **126**, 19 (1987).

19. Beneš L., Zima V., Kalousová J., Votinský J.: Collect. Czech. Chem. Commun. **59**, 1616 (1994).

20. Beneš L., Hyklová R., Kalousová J., Votinský J.: Inorg. Chim. Acta **177**, 71 (1990).

21. Martinez-Lara M., Jimenez-Lopez A., Moreno-Real L., Bruque S., Casal B., Ruiz-Hitzky E.: Mat. Res. Bull. **20**, 549 (1985).

22. Nakajima H., Matsubayashi G.: Chem. Lett. **1993**, 423.

23. Beneš L., Votinský J., áë, ová J, Handlíř K.: Inorg. Chim. Acta **176**, 255 (1990).

24. Martinez-Lara M., Moreno-Real L., Jimenez-Lopez A., Bruque-Games S., Rodriguez-Garcia A.: Mat. Res. Bull. **21**, 13 (1986).

25. Johnson J.W., Jacobson A.J., Brody J.F., Rich S.M.: Inorg. Chem. **21**, 3820 (1982).

26. Pozas-Tormo R., Moreno-Real L., Bruque-Games S., Martinez-Lara M., Ramos-Barrado J.: Mat. Sci. Forum **91-93**, 511 (1992).

27. Matsubayashi G., Nakajima H.: Chem. Lett. **1993**, 31.

28. Nakajima H., Matsubayashi G.: J. Mater. Chem. **4**, 1325 (1994).

29. DeStefanis A., Foglia S., Tomlinson A.A.G.: J. Mater. Chem. **5**, 475 (1995).

30. DeStefanis A., Tomlinson A.A.G.: J. Mater. Chem. **5**, 319 (1994).

31. Rodriguez-Castellon E., Jimenez-Lopez A., Martinez-Lara M., Moreno-Real L.: J. Incl. Phenom. **5**, 335 (1987).

32. Matsubayashi G., Ohta S.: Chem. Lett. **1990**, 787.

33. Datta A., Bhaduri S., Kelkar R. Y., Khwaja H. I.: J. Phys. Chem. **98**, 11811 (1994).

34. Jacobson A.J., Johnson J.W., Brody J.F., Scanlon J.C., Lewandowski J.T.: Inorg. Chem. **24**, 1782 (1985).

35. Jacobson A.J., Johnson J.W.: Mater. Sci. Monogr. **28A**, 469 (1985).

36. Šišková R., Beneš L., Zima V., Vlček M., Votinský J., Kalousová J.: Polyhedron **12**, 181 (1993).

37. Zima V., Beneš L., Šišková R., Fatěna P., Votinský J.: Solid State Ionics **67**, 277 (1994).

38. Zima V., Beneš L., Votinský J., Kalousová J.: Mol. Cryst. Liq. Cryst. **244**, 121 (1994).
39. Zima V., Beneš L., Votinský J., Kalousová J.: Solid State Ionics, **67**, 277 (1994).
40. Whittingham M.S., Jacobson A.J. in *Intercalation Chemistry*, p. 304, Academic Press, New York 1982.
41. Lomax J.F., Fontanella J.J., Wintersgill M.C., Kotarski A.: Mat. Res. Soc. Symp. Proc. **210**, 681 (1991).
42. Beneš L., Richtrová K., Votinský J., Kalousová J., Zima V.: Powder Diffraction **8**, 130 (1993).
43. Richtrová K., Votinský J., Kalousová J., Beneš L., Zima V.: J. Solid State Chem., **116**, 400 (1995).
44. Melánová K., Votinský J., Beneš L., Zima V.: Mat. Res. Bull., **30**, 1115 (1995).

Beneš L., Zima V./Sci. Pap. Univ. Pardubice Ser. A 2 (1996) 121-149

149